0031-3998/00/4806-0782
PEDIATRIC RESEARCH

Vol. 48, No. 6, 2000
Printed in U.S.A.

Antenatal Endotoxin and Glucocorticoid Effects on Lung Morphometry in Preterm Lambs

KAREN E. WILLET, ALAN H. JOBE, MACHIKO IKEGAMI, JOHN NEWNHAM, SIOBHAIN BRENNAN, AND PETER D. SLY

Division of Clinical Sciences, Telethon Institute for Child Health Research, Perth, Australia [K.E.W., S.B., P.D.S.]; Division of Pulmonary Biology, Children's Hospital Medical Center, Cincinnati, Ohio, U.S.A. [A.H.J., M.I.]; Women and Infants Research Foundation, University of Western Australia at King Edward Memorial Hospital, Perth, Australia [J.N.]; and Department of Pediatrics, University of Western Australia at Princess Margaret Hospital, Perth, Australia [P.D.S.]

ABSTRACT

In utero inflammation may accelerate fetal lung maturation but may also play a role in the pathogenesis of chronic lung disease. We examined the impact of endotoxin, a potent proinflammatory stimulus, on structural and functional maturation of preterm sheep lungs. Date bred ewes received 20 mg *Escherichia coli* endotoxin or saline by ultrasound guided intra-amniotic injection at 119 d gestation. A comparison group of animals received 0.5 mg/kg betamethasone, a known maturational agent, at 118 d gestation. Lambs were delivered by cesarean section at 125 d (term = 150 d) and ventilated for 40 min. Lung function data are reported elsewhere. Total and differential white cell counts were performed on amniotic fluid and fetal lung fluid samples. Morphometric analyses were performed on inflation fixed right upper lobes. Total cell count increased slightly but not significantly in both amniotic fluid and fetal lung fluid. Both endotoxin and betamethasone had similar effects on alveolarization: average alveolar volume increased by approximately 20% and total alveolar number decreased by almost 30%. Both treatments led to thinning of alveolar walls, although this was statistically significant in the betamethasone-treated group only. Although antenatal endotoxin leads to striking improvements in postnatal lung function, this may be at the expense of normal alveolar development. **(*Pediatr Res* 48: 782–788, 2000)**

Abbreviations

RDS, respiratory distress syndrome
BPD, bronchopulmonary dysplasia
PEEP, positive end expiratory pressure
RUL, right upper lobe
FLV, fixed lobe volume
PF, volume fraction of lung parenchyma
S_V, surface area per unit volume of alveoli and alveolar ducts

RDS is a major cause of morbidity and mortality in preterm neonates (1). Although most infants who develop RDS will recover, up to 20% will subsequently develop BPD (2). BPD has traditionally been attributed to barotrauma and oxidant injury, associated with prolonged mechanical ventilation and supplemental oxygen support (3), however, there is mounting evidence to suggest that perinatal inflammation may play a vital role in the pathogenesis of chronic lung disease. Elevated levels of the proinflammatory cytokines IL-6, IL-8, and IL-1β in amniotic fluid are strongly predictive of BPD in preterm neonates delivered within 5 d of amniocentesis (4). Tracheal lavage neutrophil count and elastase activity are significantly higher during the first week of life in intubated neonates who subsequently develop BPD, compared with those who do not develop BPD (5, 6). Paradoxically, a number of clinical and animal-based studies suggest that antenatal exposure to inflammatory mediators may accelerate fetal lung maturation. Watterberg *et al.* reported that infants exposed prenatally to chorioamnionitis had elevated lavage IL-1β from d 1 and an increased risk of developing BPD, despite having a decreased incidence of RDS (7). Antenatal exposure to IL-1α upregulates production of surfactant protein A (SP-A) and SP-B mRNA in fetal rabbits (8).

We hypothesized that intra-amniotic endotoxin might mature the fetal lung and we found that intra-amniotic endotoxin improved lung function after preterm birth more than did antenatal betamethasone (9). The improved lung function was associated with a 10-fold increase in the amount of surfactant lipids in alveolar lavages and 3-fold increases in lung gas volumes. A concern with any lung maturation strategy or with lung injury is that alveolarization may be suppressed. Antenatal glucocorticoids interfere with alveolarization (10), and ventilation of the preterm lung results in disrupted alveolarization in preterm ventilated baboons (11) and sheep (12) and in

Received December 16, 1999; accepted June 1, 2000.
Correspondence and reprint requests: Dr. Karen Willet, TVW Telethon Institute for Child Health Research, Roberts Rd., Subiaco 6008, PO Box 855, West Perth 6872, Australia.
Supported by grant HD-12714 from the National Institute of Child Health and Human Development and the Women and Infants Research Foundation, Perth, Australia.

infants that die of BPD (13). For this study, we hypothesized that the early lung maturation resulting from endotoxin would be associated with a disruption in alveolarization. We have compared the effects of intra-amniotic endotoxin with antenatal betamethasone on lung morphometry.

METHODS

Fetal treatment. Protocols were approved by the Animal Ethics Committees at the Children's Hospital Medical Center in Cincinnati and the Western Australian Department of Agriculture. Date bred Merino ewes were randomized to receive 20 mg of *Escherichia coli* 055:B5 endotoxin (Difco, Sparks, MD, U.S.A.; 10 mg/mL in saline) or saline by ultrasound guided intra-amniotic injection at 119 d gestation. A comparison group of animals was randomized to receive 0.5 mg/kg betamethasone (Celestone Chronodose; Schering, NSW, Australia) or saline by maternal intramuscular injection at 118 d gestation. This betamethasone dose and a 7-d treatment-to-delivery interval has previously been shown to improve postnatal lung function in preterm lambs (14).

At 125 d gestation ewes were sedated, the fetal head was exposed through midline abdominal and uterine incisions, a tracheotomy was performed, and a 4.5-mm endotracheal tube was secured in place (15). Samples of amniotic and fetal lung fluid were collected for total and differential cell counts. Animals were delivered and the umbilical cord cut.

Postnatal measurements. Following delivery, lambs were weighed, dried, and placed on infant ventilators (BP200; Bournes, Riverside, CA) set to deliver 100% oxygen at a rate of 40 breaths per minute, inspiratory time 0.75 s, and PEEP 3 cm H_2O. Peak inspiratory pressure was initially set at 35 cm H_2O. Animals were ventilated for 40 min to evaluate the effect of antenatal treatment on postnatal lung function. Clinical and lung function data from these animals have been reported (9).

Morphometry. As lung maturation is known to vary between regions of the lung (16), all morphometric assessments were performed on the RUL. The RUL was fixed at a pressure of 30 cm H_2O *via* bronchial instillation of 4% phosphate-buffered paraformaldehyde. All morphometric assessments were performed blind by the same observer (K.E.W.). Measurements were made on all animals. FLV was measured by volume displacement (17). Each lobe was then cut into 5-mm serial slices and three slices were randomly chosen for morphometric examination (18). Measurements were made on each of three 5 μm hematoxylin and eosin (H&E)-stained sections per lobe.

Volume fraction of lung parenchyma (PF = alveoli and alveolar ducts), nonparenchyma (NPF = conducting airways + blood vessels + perivascular interstitium), interlobular septa (ISF, forming the distinct lobulation of the lungs), and pleura (PLF) were estimated by superimposing a linear point counting grid (464 lines/928 points) onto enlarged photographic prints of 5 μm sections. Volume fraction is equal to Pi/Pt, where Pi represents the number of test points hitting the structure of interest (*e.g.* parenchyma) and Pt is the total number of points hitting the reference space (total of all compartments). Total volumes of parenchyma and other compartments were derived from volume fraction multiplied by fixed lobe volume.

Digitized images from 10 nonoverlapping parenchymal fields were captured from each 5 μm section using a Sony 3CCD color video camera interfaced with a Leica DMLS microscope and a Macintosh 8100/80AV computer. Images were examined at a final magnification of X950. The number of points that fell on airspace and on alveolar septal tissue and the number of air/tissue tissue/air intercepts were counted by superimposing a linear point counting grid (21 lines/42 points). The surface area of alveoli and alveolar ducts per unit volume of parenchyma (S_V) was determined using the formula $S_V = 2 I_0/L_r$, where I_0 is the number of intercepts with the air tissue interface and L_r is the length of the test line within the reference volume. Total alveolar surface area is equal to S_V * PF * FLV. Alveolar wall thickness was determined as volume per unit area of alveolar surface according to the formula AWF/S_V, where AWF is the volume fraction of alveolar wall tissue. Alveolar number per unit volume (N_V) was calculated according to the method of Weibel (19) using the equation:

$$N_V = N_A^{3/2}/(B * AF^{1/2})* D \quad (1)$$

where N_A = number of alveoli per unit area, AF = volume fraction of alveolar airspace (estimated by point counting at X950), both determined on digitized images, B = shape constant describing alveolar shape (1.55), and D = distribution variable of the characteristic linear dimension of the alveoli (= 1). In transverse section, alveoli were identified as those structures opening onto a common airspace (alveolar duct). In cross-section, alveoli were defined as those structures wholly enclosed by respiratory epithelium. Relative size and the presence of secondary alveolar septa distinguished alveolar ducts from alveoli. Size and morphology (wall thickness and cellularity) were used to distinguish alveoli from saccules. Ambiguous structures were rejected. Total number of alveoli (N_T) in the right upper lobe was calculated by multiplying lobe volume by N_V. Average alveolar volume (V_A) was calculated by dividing total alveolar volume (FLV * PF * AF) by total alveolar number.

Total and differential cell counts. Amniotic and lung fluid samples were centrifuged at 167 g for 5 min. Supernatants were removed and cell pellets re-suspended in 1 mL PBS. One aliquot (100 μL) was reserved for cytopreparations and the remaining suspension used to determine total white cell count using a hemocytometer. Fifty-microliter aliquots were centrifuged onto glass slides in a cytocentrifuge at 167 g for 5 min. Once dry, the cytospins were stained with Leishman's stain (BDH, Poole, U.K.) to enable identification of different cell types. Two to three hundred cells were counted and different cell populations were expressed as a percentage of total count.

Statistical analyses. The effect of antenatal treatment on morphometric parameters was examined by one-way ANOVA. Where the difference between treatment groups was significant, posthoc pairwise comparisons between the control group and individual treatment groups were performed using Dunnett's multiple comparison test. Total cell counts in control and endotoxin-treated animals were compared by unpaired *t* test, and differential cell counts were compared using Mann-

Whitney rank sum test. Statistical significance was accepted at $p < 0.05$.

RESULTS

Postnatal outcome. Growth and lung function data in these animals have been reported in detail (9), however, a brief summary is included for completeness (Table 1). Average birth weight was 14% lower in the betamethasone-treated group but was not affected by intra-amniotic endotoxin. Both betamethasone and endotoxin treatment resulted in significant improvements in postnatal lung function. Endotoxin treatment led to a 50% increase in compliance and a 100% increase in lung gas volume (V_{40}). The response to betamethasone treatment was less pronounced, with only a 50% increase in V_{40} ($p < 0.05$).

Lung morphometry. Fixed lobe volume and parenchymal volume were similar in control and treated animals (Table 2). However, both endotoxin and betamethasone treatment reduced the volume of interstitial tissue: interlobular septal volume decreased by 50% in endotoxin treated animals ($p < 0.05$) and pleural volume decreased by a similar amount in betamethasone treated animals ($p < 0.05$; Table 2). Nonparenchymal volume was also significantly reduced in endotoxin-treated animals ($p < 0.05$).

At 118–119 d gestation, when antenatal treatments were administered, alveolar formation was clearly well underway in the fetal sheep lung (Fig. 1). Those animals exposed to endotoxin or betamethasone before delivery at 125 d gestation had larger alveoli with slightly thinner walls than control animals (Fig. 2). Lung parenchyma comprises alveolar wall tissue, alveolar airspace, and alveolar duct space. Alveolar ducts represented the largest proportion, or volume fraction, of parenchyma at 40–50% (Table 2). Volume fraction of alveolar ducts was 10–15% higher in endotoxin- and betamethasone-treated groups compared with controls ($p < 0.05$ for both treatment groups *versus* control). Conversely, volume fraction of alveolar wall tissue was 10–15% lower in endotoxin- and betamethasone-treated animals compared with controls ($p < 0.05$ for both groups *versus* control). The volume fraction of alveolar airspace represented 25–30% of parenchyma and did not change with treatment (Table 2).

Alveolar wall thickness averaged 3.4 μm in control animals and about 10% less in treated animals, however, this difference was statistically significant only in the betamethasone-treated group ($p < 0.05$; Table 2). Alveolar surface area per unit volume (surface fraction) did not change significantly with treatment. Total alveolar surface area of the RUL averaged 15–20% greater in the control group compared with either treated group, but this difference was not statistically significant (Table 2).

Average alveolar volume was 20% greater in both the betamethasone- and endotoxin-treated groups than in the control group ($p < 0.05$ for both treated groups *versus* control; Fig. 3). As a result of the increase in alveolar volume, alveolar numerical density (number per unit volume) was 20–30% lower in treated animals, although this difference was statistically significant in the endotoxin group only ($p < 0.05$; Fig. 3). Total alveolar number averaged 550 million in the control group and about 30% less in both the endotoxin- and betamethasone-treated groups ($p < 0.05$ *versus* control, Fig. 3).

Total and differential cell counts. Cell counts were performed on five control and five endotoxin-treated animals. Endotoxin exposure was characterized primarily by a significant influx of neutrophils and, to a lesser extent, macrophages (Table 3). The pattern of cellular influx was similar in amniotic and fetal lung fluid. Total white cell count in both the amniotic and fetal lung fluid increased with endotoxin treatment, although the differences were not statistically significant (Table 3).

DISCUSSION

We examined changes in lung structure after intra-uterine exposure to the proinflammatory stimulus endotoxin, and compared these with structural changes associated with the potent lung maturational agent betamethasone. Both agents induced significant structural changes in the lung parenchyma and in other compartments. The impact of intra-amniotic endotoxin on lung structure was comparable both in nature and in magnitude to that of betamethasone. The lungs of endotoxin- and betamethasone-treated animals were characterized by fewer, larger alveoli with thinner walls. In addition to these effects on alveolar structure, both antenatal treatments also caused a decrease in the volume of interstitial tissue (pleura and interlobular septa).

The most striking effect of antenatal treatments, both endotoxin and betamethasone, was a marked reduction in alveolar number. Animals were treated at 118 or 119 d gestation, when alveolar formation is already underway in fetal sheep (20). Alveolarization begins with the appearance of crests or ridges (secondary alveolar septa) on the previously smooth, thick walls of existing airspaces (21). The outgrowth of secondary septa is an active process, associated with heightened proliferation of fibroblasts and endothelial cells, and a pronounced increase in tissue mass (22). In rats, both prenatal (23) and postnatal (24) exposure to dexamethasone has been shown to profoundly inhibit alveolar septation. In a recent study, we found evidence to suggest that alveolar septation was also impaired in preterm sheep delivered 48 h after a single direct fetal injection of betamethasone (25). Burri (26) proposed that

Table 1. *Birth weight and 40-min lung function data*

Treatment	M/F	Birth weight (kg)	Compliance (mL/cm H_2O·kg)	V_{40} (mL/kg)
Control	6/8	2.66 ± 0.08	0.24 ± 0.02	22.4 ± 4.7
Endotoxin	5/5	2.58 ± 0.06	0.37 ± 0.03*	46.4 ± 4.2*
Betamethasone	9/1	2.30 ± 0.09*	0.30 ± 0.03	34.3 ± 6.0*

V_{40}, lung volume at pressure of 40 cm H_2O.
* $p < 0.05$ vs. control.

Table 2. *Lung morphometry*

	Control (n = 14)	Endotoxin (n = 10)	Betamethasone (n = 10)
Fixed lobe volume (mL)	14.3 ± 0.6	12.9 ± 0.7	13.5 ± 0.8
Parenchymal volume (mL)	10.2 ± 0.5	10.0 ± 0.7	10.1 ± 0.7
Nonparenchymal volume (mL)	2.2 ± 0.1	1.7 ± 0.1*	2.0 ± 0.2
Interlobular septal volume (mL)	1.6 ± 0.1	0.84 ± 0.07*	1.2 ± 0.2
Pleural volume (mL)	0.37 ± 0.02	0.27 ± 0.03	0.18 ± 0.04*
Alveolar wall volume fraction (%)	29.6 ± 0.8	24.8 ± 0.9*	25.6 ± 1.3*
Alveolar airspace volume fraction (%)	28.3 ± 0.5	26.5 ± 0.8	28.7 ± 0.8
Alveolar duct volume fraction (%)	42.1 ± 1.1	48.7 ± 0.8*	45.7 ± 1.7*
Alveolar wall thickness (μm)	3.4 ± 0.1	3.1 ± 0.1	3.0 ± 0.1*
Surface fraction (mm^2/mm^3)	87.2 ± 2.0	80.0 ± 2.5	83.7 ± 2.6
Total surface area (mm^2)	2374 ± 138	2037 ± 38	1918 ± 159

Data represent mean ± SEM.
* $p < 0.05$ vs. control group.

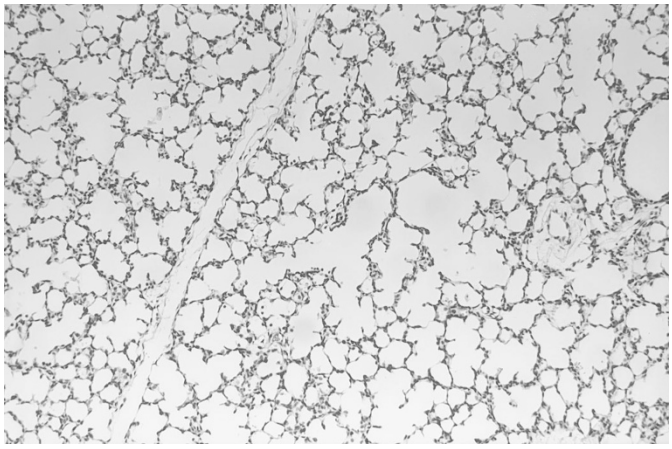

Figure 1. Light micrograph of H&E-stained 5-μm section of lung parenchyma: unventilated control animal at 119 d gestation (#99–52). Alveolar formation is clearly well established, with numerous secondary alveolar septa forming along the walls of alveolar ducts. Original magnification 120X.

the formation of secondary alveolar septa is possible only when the supporting primary septa is "immature" and that glucocorticoids, by promoting precocious differentiation of alveolar epithelial cells, abolish the ability of these cells to proliferate and form secondary alveolar septa. It is interesting to note that despite impaired alveolar development, the lungs of betamethasone-treated animals are functionally superior to those of control animals (9), an observation that points to a complex relationship between acinar structure and lung function.

We anticipated that endotoxin exposure, resulting in a proinflammatory response in the fetal lung, might interfere with alveolarization. Two general mechanisms are possible. Endotoxin could "stress" the fetus and elevate fetal cortisol resulting in clinical lung maturation and decreased alveolarization. This is the sequence suggested by Watterberg *et al.* (27) for preterm infants that are exposed to amnionitis and have a lower risk of RDS but an increased risk of BPD. However, these animals had low cord plasma cortisol levels (9) and we have other measurements indicating no elevations of fetal plasma cortisol values for times from 5 h to 7 d after intra-amniotic endotoxin (unpublished data). The other possibility is that proinflammatory cytokine elevations can disrupt alveolarization. Transgenic mice that overexpress IL-6, IL-11, TNF-α or TGFα in the lung epithelium have poor alveolarization (28–31), and infants developing BPD have chronically elevated proinflammatory cytokines in airway samples (32).

Estimation of alveolar number from two-dimensional sections may be associated with errors relating to differences in alveolar size (33). The probability of a structure appearing in any two-dimensional plane is proportional to its height. The larger an alveolus, the greater the probability it will be counted (*i.e.* counting is biased in favor of larger structures). Because both endotoxin- and betamethasone-treated animals had larger alveoli than their control counterparts, alveolar number may have been overestimated in treated animals, thus lessening the apparent effect of treatment on alveolarization. Similarly, assumptions about alveolar shape may also lead to errors in estimates of alveolar number (19). The shape coefficient (β) relates volume to cross-sectional area, and is inversely related to ϵ, the ratio of diameter to length (height) (19). Weibel estimated a value of 1.55 for β in mature alveoli. In immature (shallow) alveoli, where the ratio of diameter to height is larger (*i.e.* ϵ increases), β would be expected to be smaller. Using a shape coefficient of 1.55 in immature lungs may lead to an overestimation of alveolar number, although it is not possible to determine the extent of this effect. There are no published data in immature lungs either estimating an alveolar shape constant or examining the appropriateness of $\beta = 1.55$.

In addition to changes in the gas exchange region of the lung, antenatal endotoxin also led to a significant reduction in nonparenchymal volume. It is unlikely that endotoxin treatment interferes with airway and/or vascular development *per se*: the decrease in nonparenchymal volume more likely reflects a decrease in perivascular interstitium. Following birth, fetal lung liquid is rapidly absorbed from the alveolar lumen, temporarily pooling in the lung interstitium (perivascular space, interlobular septa and pleura) before being cleared from the lung *via* the pulmonary circulation (34). During the first 20 min after birth, some 50–80% of fluid volume disappears from the airspaces (35). In term rabbits, volume of perivascular "cuffs" peaks at 30 min postdelivery (36), decreasing to prenatal size within 2–4 h. In the present study, lung fixation probably coincided with peak interstitial pooling of lung liquid. Reduced nonparenchymal volume after 40 min of ventilation may indicate decreased interstitial pooling in endotoxin-treated animals.

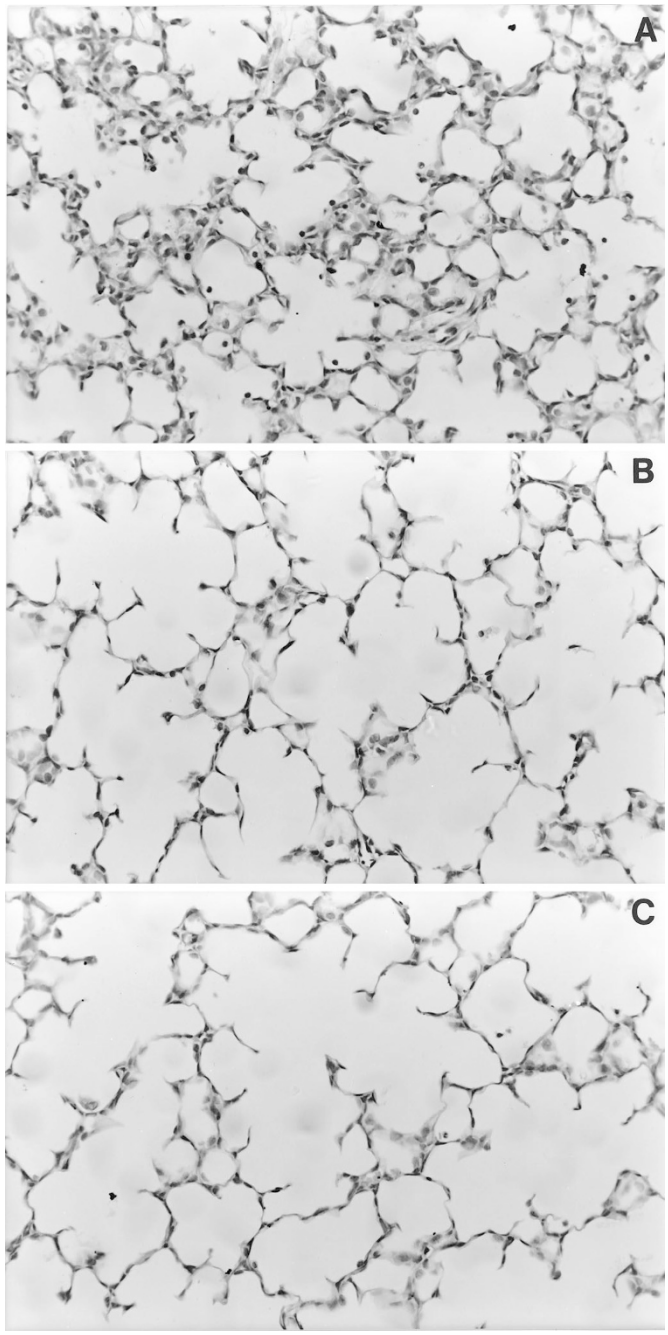

Figure 2. Light micrographs of H&E-stained 5-μm sections of lung parenchyma: animals delivered at 125 d and ventilated for 40 min. *Panel A*: Control animal (#98–11). *Panel B*: Endotoxin-treated animal (#98–125). *Panel C*: Betamethasone-treated animal (#98–30). Lung samples from control animals had smaller alveoli with slightly thicker walls compared with lung samples from endotoxin- or betamethasone-treated animals. Original magnification 300X.

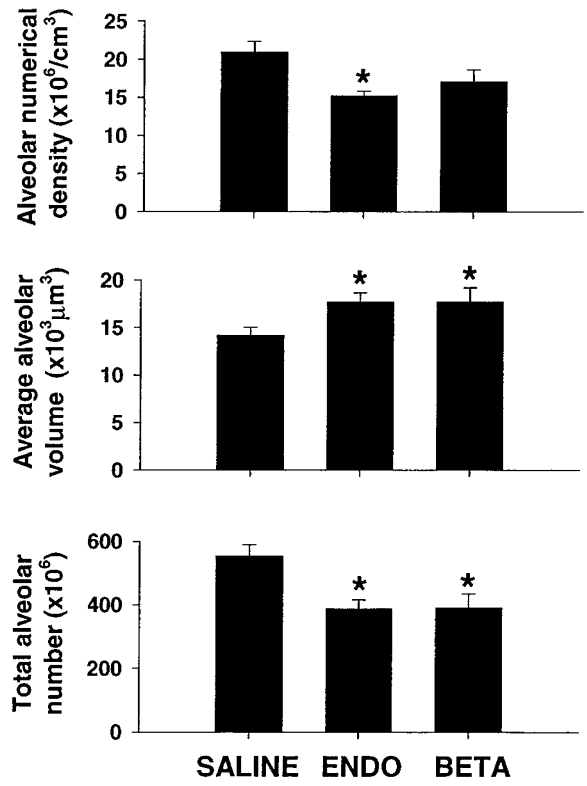

Figure 3. Alveolar number and volume. Values represent group mean ± SEM for control (saline) and endotoxin- (endo) and betamethasone- (beta) treated animals. *Panel A*: Alveolar number per unit volume of parenchymal tissue. *Panel B*: Average alveolar volume. *Panel C*: Total alveolar number in the right upper lobe. Significant increase in alveolar volume and decrease in both alveolar numerical density and total alveolar number with endotoxin treatment. Significant increase in alveolar volume and decrease in total alveolar number with betamethasone treatment. * $p < 0.05$.

A decrease in interlobular septal and pleural volumes is consistent with this concept. Betamethasone-treated animals also had reduced interstitial volumes, which is in agreement with previous findings in steroid treated preterm sheep (25). Decreased interstitial volume may reflect more rapid clearance of lung liquid from the interstitium in treated animals. Different rates of fluid clearance may partly contribute to the improvement in postnatal lung function with antenatal treatment. Variability in the volume of lung fluid in the airspaces, and perhaps to a lesser extent in the lung interstitium, will impact on lung function. There are no published data examining the impact of antenatal interventions on the kinetics of postnatal fetal lung liquid clearance during mechanical ventilation following preterm birth.

Animals were ventilated for a period of 40 min following delivery, during which lung function was determined (9). Despite comparable lung structure, the lungs of endotoxin-treated animals were functionally better than those of betamethasone-treated animals. The difference in lung function between the two treated groups may be due to differential effects of endotoxin and betamethasone on the surfactant system. Endotoxin treatment induced an almost 10-fold increase in alveolar saturated phosphatidylcholine pool size as well as seven- to ninefold increases in SP-A and SP-B, considerably greater than the increases induced by betamethasone (9). Findings from a number of previous studies by our group suggest that glucocorticoids improve lung function both by accelerating structural maturation (37) and by increasing production and secretion of surfactant (38), the predominant influence on lung function at the time of delivery depending on the treatment to delivery interval. In the present study, where delivery occurred 6–7 d after treatment, effects on the surfactant system may be the predominant influence on lung function.

Table 3. *Total and differential cell counts in amniotic and fetal lung fluid*

	Total cell count ($\times 10^6$/mL)	Differential cell count (%)				
		EPI	NPH	EOS	LYMPH	MACRO
Fetal lung fluid						
Control ($n = 5$)	0.93 ± 0.47	93.0	1.0	0.0	0.0	3.0
Endotoxin ($n = 5$)	1.93 ± 0.58	6.0*	79.0*	0.0	1.8	13.0
Amniotic fluid						
Control ($n = 5$)	0.27 ± 0.12	98.5	0.0	0.0	0.3	0.3
Endotoxin ($n = 5$)	0.54 ± 0.14	22.0*	57.0*	0.0	2.0	7.5*

Total cell count values represent group mean ± SEM. Differential cell counts represent median values. EPI, epithelial cells; NPH, neutrophils; EOS, eosinophils; LYMPH, lymphocytes; MACRO, macrophages.

* $p < 0.05$ vs. control by Mann-Whitney rank sum test.

The time course of the systemic inflammatory response to endotoxin administration is well characterized in adult animals, although there is not much information about fetal responses. In adult animals, significant neutrophil sequestration is evident in the lungs within 6 h of exposure (39). At this time point, the migrating neutrophils are almost solely confined to the vasculature. The cellular influx peaks by around 24 h and, at this time, neutrophils are seen in both the interstitium and in the airspaces (39). By 48 h almost all neutrophils are recoverable by bronchoalveolar lavage (40). Our findings are consistent with this pattern: we found neutrophils in peripheral airspaces of endotoxin-treated animals, although there were no inflammatory cells in alveolar or airway walls and there was no evidence of overt inflammatory changes in the lung tissue (9).

Although there is evidence to suggest that perinatal inflammation plays a role in development of BPD in very preterm infants, there is also mounting evidence to suggest that intrauterine exposure to inflammatory stimuli may accelerate fetal lung maturation before delivery. Our findings in preterm sheep support this argument. Although antenatal endotoxin exposure leads to greatly increased production of surfactant components and a striking improvement in postnatal lung function, as is thought to be the case with antenatal glucocorticoids, these maturational changes may occur at the expense of normal alveolar development.

REFERENCES

1. Guyer B, Martin JA, MacDorman MF, Anderson RN, Strobino DM 1997 Annual summary of vital statistics—1996. Pediatrics 100:905–918
2. Stevenson DK, Wright LL, Lemons JA, Oh W, Korones SB, Papile LA, Bauer CR, Stoll BJ, Tyson JE, Shankaran S, Fanaroff AA, Donovan EF, Ehrenkranz RA, Verter J 1998 Very low birth weight outcomes of the National Institute of Child Health and Human Development Neonatal Research Network, January 1993 through December 1994. Am J Obstet Gynecol 179:1632–1639
3. O'Brodovich HM, Mellins RB 1985 Bronchopulmonary dysplasia. Unresolved neonatal acute lung injury. Am Rev Respir Dis 132:694–709
4. Yoon BH, Romero R, Jun JK, Park KH, Park JD, Ghezzi F, Kim BI 1997 Amniotic fluid cytokines (interleukin-6, tumor necrosis factor-alpha, interleukin-1 beta, and interleukin-8) and the risk for the development of bronchopulmonary dysplasia. Am J Obstet Gynecol 177:825–830
5. Merritt TA, Cochrane CG, Holcomb K, Bohl B, Hallman M, Strayer D, Edwards DK, Gluck L 1983 Elastase and alpha 1-proteinase inhibitor activity in tracheal aspirates during respiratory distress syndrome. Role of inflammation in the pathogenesis of bronchopulmonary dysplasia. J Clin Invest 72:656–666
6. Watterberg KL, Carmichael DF, Gerdes JS, Werner S, Backstrom C, Murphy S 1994 Secretory leukocyte protease inhibitor and lung inflammation in developing bronchopulmonary dysplasia. J Pediatr 125:264–269
7. Watterberg KL, Demers LM, Scott SM, Murphy S 1996 Chorioamnionitis and early lung inflammation in infants in whom bronchopulmonary dysplasia develops. Pediatrics 97:210–215
8. Bry K, Lappalainen U, Hallman M 1997 Intramaniotic interleukin-1 accelerates surfactant protein synthesis in fetal rabbits and improves lung stability after premature birth. J Clin Invest 99:2992–2999
9. Jobe AH, Newnham JP, Willet KE, Sly P, Ervin MG, Bachurski C, Possmayer F, Hallman M, Ikegami M 2000 Antenatal endotoxin and glucocorticoid effects on the lungs of preterm lambs. Am J Obstet Gynecol 182:401–408
10. Massaro GD, Massaro D 1996 Formation of pulmonary alveoli and gas-exchange surface area: quantitation and regulation. An Rev Physiol 58:73–92
11. Coalson JJ, Winter VT, Siler-Khodr T, Yoder BA 1999 Neonatal chronic lung disease in extremely immature baboons. Am J Resp Crit Care Med 160:1333–1346
12. Albertine KH, Jones GP, Starcher BC, Bohnsack JF, Davis PL, Cho S, Carlton DP, Bland RD 1999 Chronic lung injury in preterm lambs. Am J Respir Crit Care Med 159:945–958
13. Husain NA, Siddiqui NH, Stocker JR 1998 Pathology of arrested acinar development in postsurfactant bronchopulmonary dysplasia. Human Pathol 29:710–717
14. Ikegami M, Polk DH, Jobe AH, Newnham J, Sly P, Kohan R, Kelly R 1996 Effect of interval from fetal corticosteroid treatment to delivery on postnatal lung function of preterm lambs. J Appl Physiol 80:591–597
15. Jobe AH, Polk D, Ikegami M, Newnham J, Sly P, Kohen R, Kelly R 1993 Lung responses to ultrasound-guided fetal treatments with corticosteroids in preterm lambs. J Appl Physiol 75:2099–2105
16. Kendall JZ, Lakritz J, Plopper CG, Richards GE, Randall GC, Nagamani BN, Weir AJ 1990 The effects of hydrocortisone on lung structure in fetal lambs. J Dev Physiol 13:165–172
17. Scherle W 1970 A simple method for volumetry of organs in quantitative stereology. Mikroskopie 26:57–60
18. Bolender RP, Hyde DM, Dehoff RT 1993 Lung morphometry: a new generation of tools and experiments for organ, tissue, cell, and molecular biology. Am J Physiol 9:521–548
19. Weibel ER 1963 Morphometry of the Human Lung. Springer-Verlag, Berlin
20. Docimo SG, Crone RK, Davies P, Reid L, Retik AB, Mandell J 1991 Pulmonary development in the fetal lamb: morphometric study of the alveolar phase. Anat Rec 229:495–498
21. Burri PH 1975 The postnatal growth of the rat lung. III. Morphology Anat Rec 180:77–98
22. Kauffman SL, Burri PH, Weibel ER 1974 The postnatal growth of the rat lung. II. Autoradiography Anat Rec 180:63–76
23. Massaro GD, Massaro D 1992 Formation of alveoli in rats: postnatal effect of prenatal dexamethasone. Am J Physiol 263:37–41
24. Blanco LN, Massaro GD, Massaro D 1989 Alveolar dimensions and number: developmental and hormonal regulation. Am J Physiol 257:L240–L247
25. Willet KE, McMenamin P, Pinkerton KE, Ikegami M, Jobe AH, Gurrin L, Sly PD 1999 Lung morphometry and collagen and elastin content: changes during normal development and following prenatal hormones in sheep. Pediatr Res 45:615–625
26. Burri PH 1997 Postnatal development and growth. In: Crystal RG, West JB, Weibel ER Barnes PJ (eds) The Lung: Scientific Foundations. Philadelphia, Lippincott-Raven, pp 1013–1026
27. Watterberg KL, Scott SM, Naeye RL 1997 Chorioamnionitis, cortisol, and acute lung disease in very low birth weight infants. Pediatrics 99:E6
28. DiCosmo BF, Geba GP, Picarella D, Elias JA, Rankin JA, Stripp BR, Whitsett JA, Flavell RA 1994 Airway epithelial cell expression of interleukin-6 in transgenic mice. Uncoupling of airway inflammation and bronchial hyperreactivity. J Clin Invest 94:2028–2035
29. Miyazaki Y, Araki K, Vesin C, Garcia I, Kapanci Y, Whitsett JA, Piguet PFPV 1995 Expression of a tumor necrosis factor-alpha transgene in murine lung causes lymphocytic and fibrosing alveolitis. J Clin Invest 96:250–259
30. Hardie WD, Bruno MD, Huelsman KM, Iwamoto HS, Carrigan PE, Leikauf GD, Whitsett JA, Korfhagen TR 1997 Postnatal lung function and morphology in transgenic mice expressing transforming growth factor-alpha. Am J Pathol 151:1075–1083
31. Ray P, Tang W, Wang P, Homer R, Kuhn C, 3rd, Flavell RA, Elias JA 1997 Regulated overexpression of interleukin 11 in the lung. Use to dissociate development-dependent and -independent phenotypes. J Clin Invest 100:2501–2511
32. Groneck P, Speer CP 1995 Inflammatory mediators and bronchopulmonary dysplasia. Arch Dis Child Fetal Neo Ed 73:1–3
33. Sterio DC 1984 The unbiased estimation of number and sizes of arbitrary particles using the disector. J Microscopy 134:127–136
34. Bland RD, Hansen TN, Haberkern CM, Bressack MA, Hazinski TA, Raj JU, Goldberg RB 1982 Lung fluid balance in lambs before and after birth. J Appl Physiol 53:992–1004

35. Egan EA, Dillon WP, Zorn S 1984 Fetal lung liquid absorption and alveolar epithelial solute permeability in surfactant deficient, breathing fetal lambs. Pediatr Res 18:566–570
36. Bland RD, McMillan DD, Bressack MA, Dong LA 1980 Clearance of liquid from lungs of newborn rabbits. J Appl Physiol 49:171–177
37. Pinkerton KE, Willet KE, Peake JL, Sly PD, Jobe AH, Ikegami M 1997 Prenatal glucocorticoid and T4 effects on lung morphology in preterm lambs. Am J Resp Crit Care Med 156:624–630
38. Polk DH, Ikegami M, Jobe AH, Sly P, Kohan R, Newnham J 1997 Preterm lung function after retreatment with antenatal betamethasone in preterm lambs. Am J Obstet Gynecol 176:308–315
39. Rinaldo JE, Henson JE, Dauber JH, Henson PM 1985 Role of alveolar macrophages in endotoxin-induced neutrophilic alveolitis in rats. Tissue Cell 17:461–472
40. Venaille T, Snella MC, Holt PG, Rylander R 1989 Cell recruitment into lung wall and airways of conventional and pathogen-free guinea pigs after inhalation of endotoxin. Am Rev Respir Dis 139:1356–1360